PhD University of Edinburgh 1992

Phase-Only Optical Information Processing

D. J. Potter

Chapter 1
Phase Visualisation Techniques

Introduction

In the context of optical image processing, one frequently performs operations on the Fourier spectrum of a two dimensional scene with a view to enhancing certain aspects of that scene. Many typical scenes comprise of ordinary information such as might be contained on a photographic transparency, exhibiting a spatially varying photographic density which modulates the amplitude of an incident light beam. For instance, one might remove the zero spatial frequency of the spectrum to perform a contrast enhancing operation on the image. There exists, however, a class of objects which rely heavily on image processing operations in order that any useful information be obtainable from them at all, and these are known as *phase* objects. Phase objects present a spatially varying optical path to the incident illumination, and in real situations a slight degree of amplitude modulation usually accompanies this.

This first chapter begins with an historical introduction to the classical techniques which have been used to render the phase variations visible to the (intensity sensitive) human eye. An introduction to the terminology of optical information processing is to be found in appendix A and is briefly recapped here. Recall that under coherent illumination of an object situated in the front focal plane of a positive lens the spatial frequency spectrum appears in the back focal plane. An alternative name for the back focal plane is therefore the *frequency* plane. It should be noted that the equations relating the light field in the frequency plane to that of the object plane are also generally applicable to complex objects, of which the phase objects of concern in this thesis are a subset.

1 Historical Development of Phase Visualisation

Historically, much scientific work has been performed with two optical systems - the telescope and the microscope. Although Galileo was probably not the first to invent the refracting telescope[1], his rapid development of the instrument from 1609 has resulted in his association as the father of the telescope today. Certainly he was the first human to view the giant moons of the planet Jupiter - Io, Ganymede, Callisto and Europa - and thus dare to venture our world was not the centre of the universe.

A year later, in 1610, Galileo was working on a new but similar instrument - the microscope. The then new field of science called `microscopy' opened up the previously unsuspected world of the ultra small. Tiny life forms no larger than a pinhead were revealed, and with instrumental improvements by later scientists the existence of bacteria proven. This discovery prompted the sterilisation of surgical equipment taken for granted today, saving millions of lives since then through freedom from bacterial infection.

It is beyond doubt that the new world opened by the invention of the microscope inspired the scientists of that time to seek yet greater magnification and sharper images, to delve deeper into this tiny world. Yet technical improvement in the design of the microscope was hampered by the lack of a proper theory of image formation.

Not until the late nineteenth century, when Raleigh provided the mathematical foundations of the present day diffraction theory of imaging was the microscope properly understood. A full account of this development may be found in [1, pages 370-371].

1.1 Zernike's Analysis

The work of this thesis has its roots in the developments of the early twentieth century microscopists. For many years they had observed tiny, transparent organisms and sought ways to improve the visibility of these creatures so that their nature might better be understood. The problem was solved by F.Zernike in 1935 [1, page 425] when he considered the way the organisms altered the phase of the illuminating light field.

By the correct positioning of a thin phase-plate in the back focal plane of the microscope objective, Zernike demonstrated that optical thickness variations of the organism may be rendered visible as intensity variations. Organisms of this kind are described today as `phase' objects, as they alter only the optical path of the illumination but not the amplitude. Although phase visualisation techniques did exist prior to Zernike's method, their fundamental drawback was in failure to produce an image whose structure could readily be identified with the structure of the phase object.

In his original publication of 1934 [2], Fritz Zernike proposed that his technique, known as `phase contrast', be applied to enhance an existing test - the `knife edge test' - on the optical quality of astronomical mirrors [3]. A year later he followed this work with a publication on applying the principles of phase contrast to the imaging of transparent organisms under the microscope [4]. A most explanatory review paper published in 1942 by Zernike [5] reviews both the phase contrast method and several previous imaging methods. This paper forms the basis of the present section, serving as a concise introduction to the subject.

In this thesis the analysis of Zernike is conducted with reference to a coherent optical processor, such as described in appendix A. The object plane transmittance g(x,y) may be written

$$g(x,y) = R(x,y)\, e^{if(x,y)} \tag{1}$$

where both R(x,y) and f(x,y) are wholly real and respectively describe the variations in amplitude and optical path which the object presents to an illuminating light field. For the following analysis to apply the illumination is required to be at least partially (and at best completely) coherent in order that it be possible to associate a particular phase to the light field at a specified location in space.[2]

Zernike's analysis is most readily performed on a 1-D periodic object which will allow the use of a Fourier series approach. A review of the mathematics of both one and two dimensional Fourier series may be found in appendix B. The series representation of a general function g(x) is given as

$$g_s(x) = \sum_{m=-\infty}^{\infty} c_m\, e^{i\, mx} \tag{2}$$

where

$$c_m = \frac{1}{2\pi} \int_{-\pi}^{\pi} g(x)\, e^{-i\, mx}\, dx \tag{3}$$

In general, periodic objects are termed `gratings' in optics and two such gratings are of interest here. An *amplitude* grating exibits variations in amplitude across its extent but none in optical depth, whereas a *phase* grating has constant amplitude transmittance (usually unity) with a spatially varying optical depth.

The simplest form of either grating consists of equally spaced regions of alternating attenuation / retardation, described by a square wave function. Both gratings cause diffraction of an incident light field and it is mathematically sound to view the diffracted field as a superposition of plane waves, each wave making an angle θ_m with the optical axis of the system (Appendix A, Fig A.3). Each wave is imaged by the transform lens to the corresponding spectral order m in the frequency plane. This is a consequence of the fact that a periodic object

requires only *discrete* spatial frequencies in order that it be synthesised. Hence, the frequency plane consists of discrete spectral orders, with amplitude c_m, rather than a continuous distribution of spatial frequencies. The image field is the Fourier Transform of the light distribution in the frequency plane, G(ν), which in this case reduces to a Fourier series of form

$$G(\nu) = \sum_{m=-\infty}^{\infty} c_m \, \delta(\nu - m) \qquad (4)$$

where δ denotes the dirac delta function. The equations introduced in this section form the basis of a mathematical interpretation of phase visualisation techniques.

1.2 The Schlieren Method

The principle of the Schlieren method is to block the negative spectral orders so that only the zero and positive orders form the resulting image. The name of the technique derives from its use in the testing of optical glass. A common occurrence was the inclusion of small amounts of glass of different refractive index, caused by molten glass dissolving a small amount of the lining of the crucible. This results in `streaks' appearing in the glass, the German word for this being `Schlieren'. In practice, the zero order light is often attenuated to increase the contrast of the resulting image [6].

Phase Grating

If the phase variations are small enough, the exponential describing a phase grating may be expanded to include only linear terms in f(x) so that

$$e^{i\,f(x)} \cong 1 + if(x) \qquad (5)$$

This equation is the mathematical expression for what is commonly called the `weak phase approximation' and it is reasoned [7, page 491] that the weak phase approximation is valid for phase retardance values less than [(λ)/10] so that f(x) ≤ [(π)/5].

A mathematical interpretation of the Schlieren technique follows if this approximation for the object is used to calculate the spectral orders c_m. Insertion of equation 1.5 as the object in equation 1.3 results in spectral order amplitudes of

$$c_m = \frac{1}{2\pi} \int_{-\pi}^{+\pi} [\, 1 + if(x) \,]\, e^{-i\,mx}\, dx \qquad (6)$$

In order that the expression for c_m be manipulated more easily, the exponential in this equation is decomposed into cosine and sine functions and reduces to

$$\begin{aligned} c_m &= -b_m + ia_m \\ c_0 &= \delta(\,\nu\,) \end{aligned} \qquad (7)$$

where

$$a_m = \frac{1}{2\pi} \int_{-\pi}^{+\pi} f(x) \cos(\,mx\,)\, dx \qquad (8)$$

$$b_m = -\frac{1}{2\pi} \int_{-\pi}^{+\pi} f(x) \sin(\,mx\,)\, dx \qquad (9)$$

The reason for this particular choice of notation will become apparent when one considers the spectrum of an amplitude grating with transmittance

$$g'(x) = D + f(x) \tag{10}$$

where D is a constant equal to the mean transmittance of the grating. The complex Fourier coefficient for such an object is of form

$$\begin{aligned} c'_m &= a_m + ib_m \\ c'_0 &= D\,\delta(\nu) \end{aligned} \tag{11}$$

where a_m and b_m are as previously defined. Notice that the *intensities* of all but the zero spectral order are identical for both an amplitude grating and a low retardance phase grating. The essential difference between the two gratings is that a phase grating has a spectrum 90^o out of phase with its zero order, whereas an amplitude grating does not. Figure 1.4 of section 1.1.4 illustrates this essential difference on an Argand diagram.

The form of c'_m allows one to determine the series representation of the amplitude object as

$$g_s'(x) = \sum_{m=1}^{\infty} a_m \cos(mx) + b_m \sin(mx) \tag{12}$$

where the constant D has been dropped so that g_s' represents the *structure* of the grating alone. Similarly, inspection of c_m leads to the series representation of the phase grating as

$$\begin{aligned} g_s(x) &= 1 + 2i \sum_{m=1}^{\infty} (a_m \cos(mx) + b_m \sin(mx)) \\ &= 1 + 2i\, g_s'(x) \end{aligned} \tag{13}$$

In the absence of any spatial filtering, an aberration free optical processor will produce an inverted image $v(x_i)$ of the object field of form

$$v(x_i) = 1 + 2i\, g_s'(x_i) \tag{14}$$

where x_i denotes distance in the image plane. It will be observed that the structure of the phase grating, as expressed by equation 1.12, is contained within the imaginary part of the image field. The approximation of a grating with a small phase retardance means both a_m and b_m are small, so in squaring the expression for the image field to find the intensity we ignore terms in a_m^2 etc. The expression for the image intensity then becomes

$$|v(x_i)|^2 \cong 1 \tag{15}$$

as one would expect and no detail of the phase structure is visible. This is of course true for a phase object of *any* retardance, but the approximations used here may be likened to a perturbation analysis of the true situation which is valid for small perturbations (retardance). Equation 1.15 merely checks that the analysis agrees with the non-perturbed equations in the limit of extremely small perturbations.

In the Schlieren imaging technique, however, all orders on one half of the spectrum are blocked from reaching the image plane. The image field v_s is then given by

$$v_s(x_i) = \sum_{m=0}^{+\infty} c_m\, e^{-imx_i} \tag{16}$$

The corresponding intensity distribution is proportional to the square of this function and has form

$$|v_s(x_i)|^2 = \sum_{m=1}^{\infty} (b_m \cos(mx) - a_m \sin(mx)) \quad (17)$$

Thus an intensity variation relating to the phase object is revealed. Comparison of this image intensity with the phase structure f(x) of the object as given by equation 1.12 above shows, however, that the intensity distribution obtained with the Schlieren technique reveals an image which is akin to the spatial derivative of the phase structure. As such it is widely used in situations where gradients in phase are of importance, where its simple application provides an instant, if non-linear, visualisation of the phase object. In two dimensions, the pseudo-differentiation acts along a direction perpendicular to the edge of the filter in the frequency plane. Figure 1.1 shows an input scene which was used to digitally construct a phase object of maximum phase retardance [(π)/5]. The intensity distribution resulting from digital Schlieren filtering of the spectrum of the object is shown in figure 1.2, where the zero frequency has been heavily attenuated to increase the contrast as mentioned earlier.

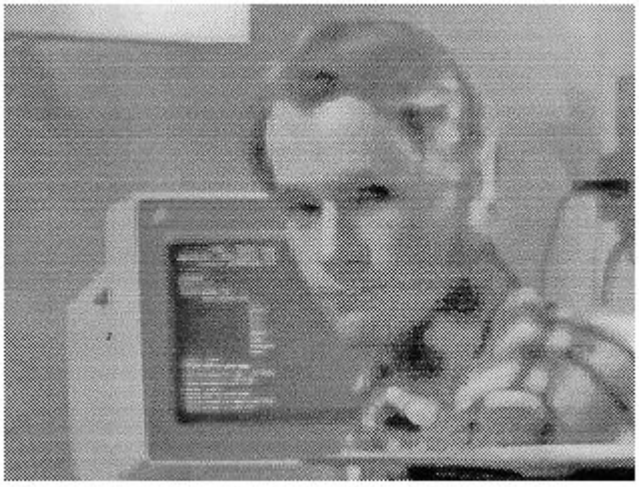

Figure 1.1: Phase object used

Figure 1.1: Phase object used

Figure 1.2: Intensity of Image after Schlieren Phase Filtering

Figure 1.2: Intensity of Image after Schlieren Phase Filtering

1.3 The Dark Ground Method

Zernike continues with an analysis of a phase visualisation technique known as the `dark ground' method, discovered in 1926 by Spierer [8]. The phase structure of the object is made visible by passing all but the central

order c_0 of the spectrum. Thus the image intensity is found to be

$$|v_s(x_i)|^2 = 4\left(\sum_{m=1}^{\infty} \left(a_m \cos(mx_i) + b_m \sin(mx_i) \right) \right)^2 \qquad (18)$$

This is the *square* of the phase structure which it is wished to know and thus is much preferable to the Schlieren method in so far as structure visualisation concerned. In the field of microscopy the process of diffraction by the object is viewed thus: the light field immediately after the object consists of both a diffracted wave and an undiffracted wave. The undiffracted wave is planar and propagates parallel to the optical axis of the system, being focussed by the transform lens to the zero order spectrum. If no object is present, the zero order spectrum is expanded by the re-transform lens to produce a uniformly illuminated field in the image plane. This is the constant or DC field spoken of in appendix A.

Figure 1.3: Intensity distribution resulting from Dark Ground Filtering

Figure 1.3: Intensity distribution resulting from Dark Ground Filtering

Removal of the zero order spectrum thus results in a dark background, all light forming the image having come from the diffracted wave only, hence the name dark (back)ground. Figure 1.3 illustrates the results of this technique via digital simulation.

1.4 The Phase Contrast Method

Zernike's insight into the problem came when he represented the light field of each order as a phasor diagram. By plotting both the field of the transmission grating along side that of the phase grating, we see that the grating orders are precisely 90^0 out of phase with the same order of the transmission grating. It struck Zernike that a much more obvious imaging method would be to rotate the vectors through 90^0, so the phase of the grating orders would appear `as an amplitude grating of exactly corresponding structure' [5].

As before, if

$$g_s'(x) = \sum_{m=1}^{+\infty} \left(a_m \cos(mx) + b_m \sin(mx) \right) \qquad (19)$$

then the grating image field which was given by

$$v(x_i) = 1 + 2i\, g_s'(x) \qquad (20)$$

now becomes

$$v(x_i) = 1 \pm 2\, g_s'(x) \qquad (21)$$

with an intensity distribution of

$$|v(x_i)|^2 \cong 1 \pm 4\, g_s'(x) \qquad (22)$$

where terms in $(g_s'(x))^2$ are small enough to be dropped. An image intensity which is directly proportional to the phase structure of the object thus results. This technique first enabled the linear visualisation of a phase object and gained Zernike the Nobel prize in 1953. The ± sign indicates that we may choose a rotation of $\pm 90^0$ of the spectra relative to the zero order. The choice of rotation sense allows us to influence whether regions of low phase retardance appear in the image as being darker than regions of higher phase retardance, or vice versa.

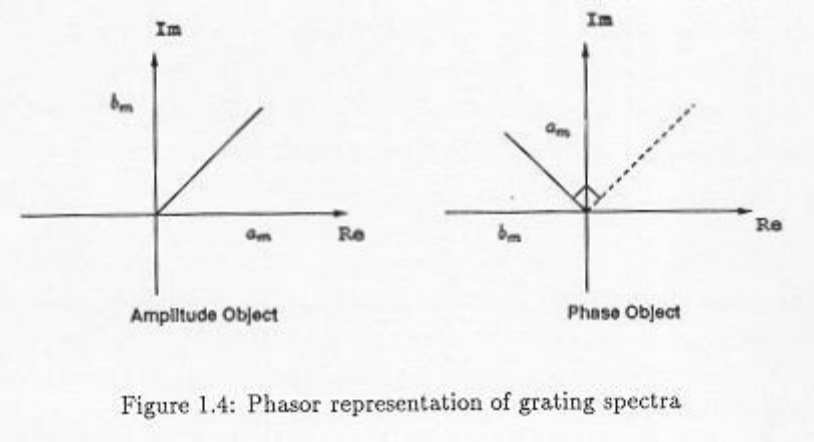

Figure 1.4: Phasor representation of grating spectra

Figure 1.4: Phasor representation of grating spectra

It is instructive to analyse this technique from a physical perspective of wave propagation. We illustrate the microscopists' view that the light field immediately after the object is comprised of both a diffracted and an undiffracted wave [9, pages 13-50]. This field may be represented by

$$\Psi = A_0 \sin(kz - \omega t + \phi) \qquad (23)$$

here A_0 is the amplitude of the incident light field, `k' is the wavenumber, $[(2\pi)/(\lambda)]$ and ω is the temporal angular frequency of the wave. The direction of propagation is along the z-axis of the system. The variable ϕ is to be taken as spatially varying and represents the phase delay of the field caused by passing through the object. As ϕ is small, we can expand this expression to obtain

$$\begin{aligned} \Psi &= A_0 \sin(\phi) \cos(kz - \omega t) + A_0 \cos(\phi) \sin(kz - \omega t) \\ &\cong A_0\, \phi \cos(kz - \omega t) \quad + \quad A_0 \sin(kz - \omega t) \end{aligned} \qquad (24)$$

The first term of equation 1.24 represents the diffracted wave and the second term the undiffracted wave. The undiffracted wave is imaged to a point in the centre of the frequency plane, and the diffracted wave to the surrounding regions of this plane. This analysis reveals that it is mathematically legitimate, for small ϕ, to view the electric field in any plane after a phase object as a sum of both an undiffracted wave and a diffracted wave.

A light wave which has propagated through regions of greater phase retardance than surrounding regions will have been slowed down slightly, spatially lagging a wave encountering no phase obstacles. This situation may be represented in our diagram if we associate such high phase retardance regions with larger, positive values of ϕ.

In order that both beams interfere to produce an image of the phase object, we must shift the diffracted wave along the z-axis either forward or backward by $[(\lambda)/4]$ relative to the undiffracted beam. Moving the diffracted beam to the left is equivalent to making it travel a greater optical path, achieved by adding a phase of $[(\pi)/2]$ in the equation of the diffracted wave. The fact that both beams are imaged to separate physical positions in the frequency plane enables this operation to be accomplished by a suitable phase filter. Figure 1.5 shows such a spatial filter for this purpose.

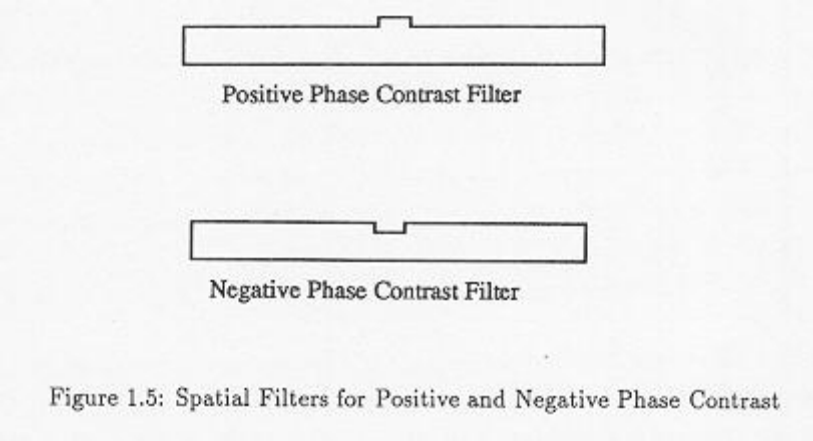

Figure 1.5: Spatial Filters for Positive and Negative Phase Contrast

Figure 1.5: Spatial Filters for Positive and Negative Phase Contrast

In the image plane, both diffracted and undiffracted beams recombine. Incorporating the effects of a [(π)/2] phase filter over the zero order of the spectrum we have an image field described by

$$\Psi = A_0 \phi \cos(kz - \omega t) + A_0 \sin(kz - \omega t + \frac{\pi}{2})$$

$$\cong A_0 (1 + \phi) \cos(kz - \omega t) \qquad (25)$$

We thus obtain a travelling wave with a spatially varying amplitude which is linearly proportional to the object phase variation. Regions of greater optical path, associated with larger ϕ values, thus appear brighter than their surrounds in this method.

Where the spectra are retarded in space relative to the zero order, as in the above analysis, regions of greater optical thickness appear brighter than their surrounds. Physical retardation of a sine wave in space is equivalent to an increase in the sine wave argument, which in the conventional phasor representation of the wave is effected by an anti-clockwise rotation of the phasor. The `sense' of rotation is mathematically called `negative', and the name of this technique is thus negative phase contrast imaging.

Spatially *advancing* the diffracted beam is equivalent to decreasing the argument of the sine wave as a whole, such a decrease being equivalent to a clockwise (or positive) rotation of the wave phasor. The resulting image is associated with the minus sign in equation 1.22, regions of higher phase thus appearing darker. This method is thus known as positive phase contrast imaging. Zernike's phase contrast methods are the usual starting point for a discussion of phase visualisation due to the ease with which the image may be described i.e. it is linearly proportional to the object phase. Although this is only true for *small* phase retardance objects, a large number of objects fall into this category and it has found widespread use in a device first patented by the German firm of Zeiss [10] known as the `phase contrast microscope'.

1.5 Taylor's Modification

We note that the image contrast may be considerably improved by the attenuation of the zero order spectrum together with the relevant phase delay. The first practical design of a phase contrast microscope also exhibiting variable zero order attenuation was described by Taylor [11] in 1947. In place of a point light source it is preferable, for increased resolution, to use an annular source of illumination - the undeviated beam in the above discussion now being imaged onto an *annular* phase plate in the rear focal plane of the microscope objective.

In Taylor's microscope, the annular phase plate is placed after a disc consisting of right handed optically active quartz. In this disc an annulus of left handed quartz is inserted so that light passing through the annular phase plate also passes through this left handed quartz plate. Although of opposite sense, the angular rotation of both quartz plates is 45^0.

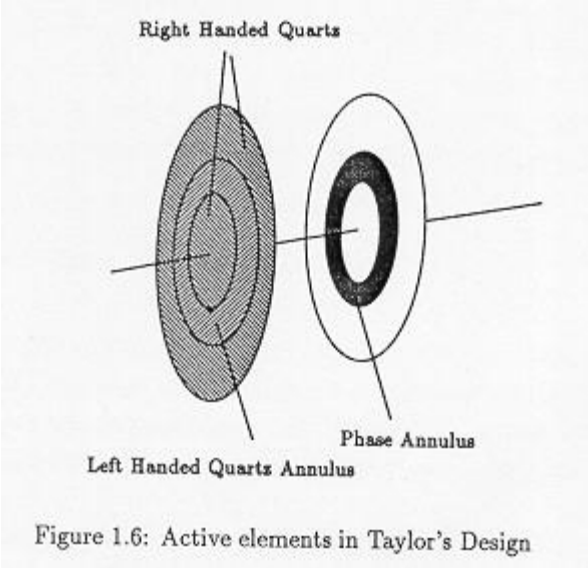

Figure 1.6: Active elements in Taylor's Design

Figure 1.6: Active elements in Taylor's Design

Linearly polarised illumination is used, the object being viewed with a rotatable analyser placed between the phase plate and the eyepiece. If the vibration direction of the analyser is set parallel to that of light emerging from the central disc and outer annulus, light from the phase plate is completely extinguished while the diffracted beam intensity is at a maximum. This corresponds to the conditions of dark ground illumination. Rotation of the analyser slightly allows some light from the phase plate to reach the image and phase contrast effects are observed. The light contribution from the phase plate can be varied by rotation of the analyser thus altering the image contrast. Once an analyser rotation of 90^0 has been effected no light from the diffracted beam is transmitted. If the phase contrast effects over this quadrant of rotation have been positive, they reverse and become negative over the next 90^0 rotation and so on until a full 360^0 rotation has been accomplished.

2 Other Phase Visualisation Techniques

A comprehensive review of all the current phase visualisation techniques is outwith the scope of this thesis. In the remaining part of this chapter we introduce the idea of interferometric visualisation techniques and end with a very recent technique capable of linearly imaging even very high phase retardance objects.

2.1 The Differential Interferometer

This device incorporates a birefringent optical element which produces two slightly displaced images. The resultant interference between these images results in the outline of the phase image becoming visible. The birefringent element is typically a Savart Polariscope [12, pages 43-46] whose operation we now discuss.

The Savart Polariscope consists of two birefringent plates, each cut with their optical axis at 45^0 to the larger plate surface as shown in fig 1.7. In this figure the double headed arrow represents the optical axis in each plate. The second plate rotated by 90^0 with respect to the first. Light entering the first plate is split into two - the ordinary and extraordinary rays O and E - and upon entering the second plate the O ray of the first plate becomes the E ray of the second plate because of the rotation of the second plate. Correspondingly, the E ray of the first plate becomes the O ray of the second plate.

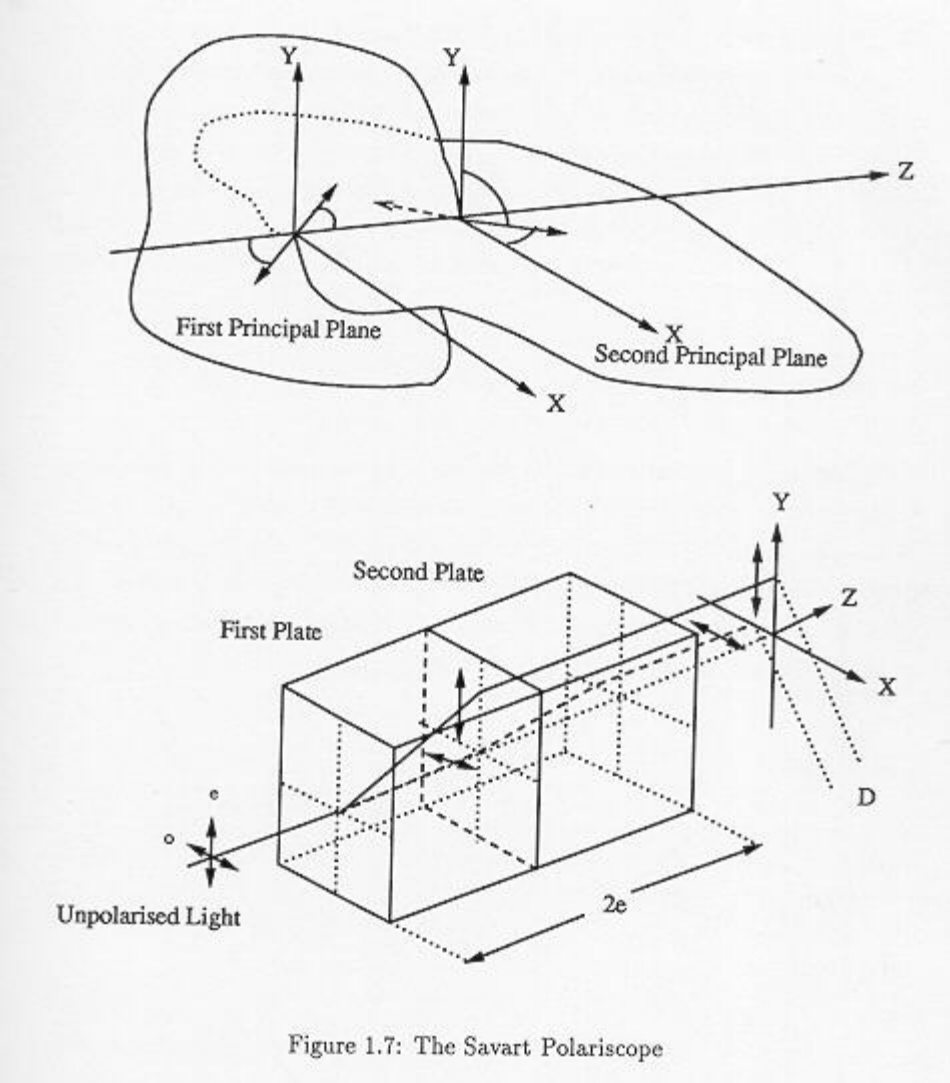

Figure 1.7: The Savart Polariscope

Figure 1.7: The Savart Polariscope

A single beam of unpolarised light entering the device thus emerges as two laterally displaced beams of light each having an orthogonal polarisation state to the other. It can be shown [] that the lateral displacement of the two beams, for a polariscope of thickness 2e, is given by

$$D = e\sqrt{2}\,\frac{n_e^2 - n_o^2}{n_e^2 + n_o^2} \qquad (26)$$

There is also a displacement of the two emerging wavefronts Δ along the direction of propagation caused by the difference in optical paths traversed by each.

We may illustrate the operation of the polariscope in figure 1.8 which shows the optical layout of a differential interferometer. A plane wave is linearly polarised by polariser P_1 and passes through the phase object which in our example is a transparent plate having a small indentation in the centre. If the wave front is described by Σ immediately after the object, it is split by the polariscope into two laterally shifted wave fronts of orthogonal polarisation Σ_1 and Σ_2.

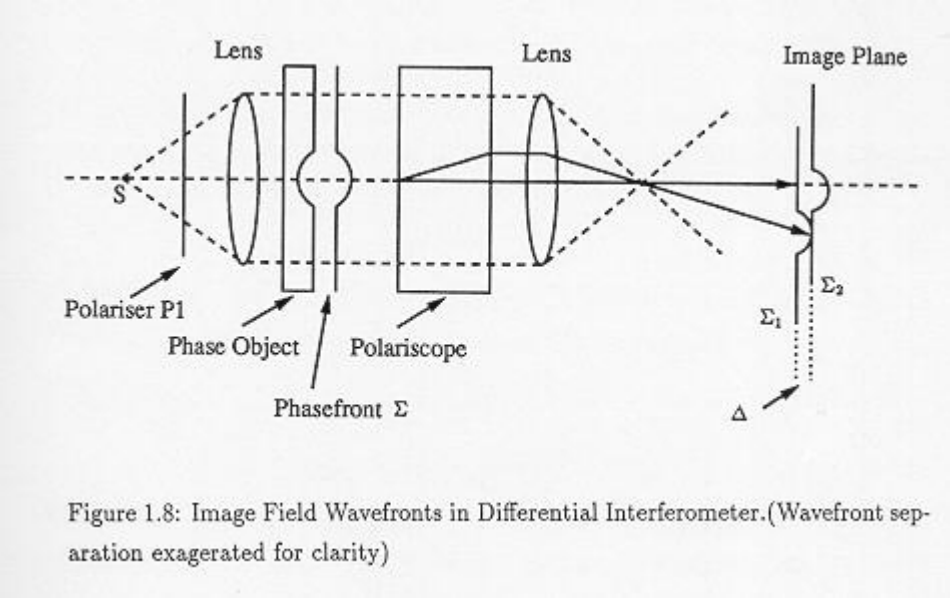

Figure 1.8: Image Field Wavefronts in Differential Interferometer.(Wavefront separation exagerated for clarity)

Figure 1.8: Image Field Wavefronts in Differential Interferometer.(Wavefront separation exagerated for clarity)

The lateral shear of both images produces interference between the two beams, with the result that the outline of the phase object is revealed. Δ is adjusted (usually by a slight tilt of the polariscope) so that the plane regions of Σ_1 and Σ_2 destructively interfere and appear dark, the interference being rendered visible by positioning an output polariser before the eyepiece. From equation 1.26 it will be noted that the lateral displacement of Σ_1 and Σ_2 may be controlled by altering the thickness of the polariscope plates. It is common practice to set the lateral displacement of the beams to be close to the resolution limit of the system so that it appears that the lateral doubling is not present. As the method gives not the optical path itself but its variations, it is known as a *differential* method.

2.2 Dyson's Interference Microscope

This device consists of two optical flats F_1 and F_2, each face being semi-silvered as in figure 1.9, and a further description may be found in [6, page 293]. Flat F_2 has an additional central region C_1 which is heavily silvered. The phase object O is placed between the flats and is illuminated by a converging beam of light. In the figure, the ray is partially reflected by the upper surface of C_2, reflected from C_1 and interferes with the ray through O that has undergone similar reflections in C_1. By using a spherical reflector with a hole in the centre, the interference between both rays can be viewed through the microscope objective and the object shows up as a distortion of a set of interference fringes.

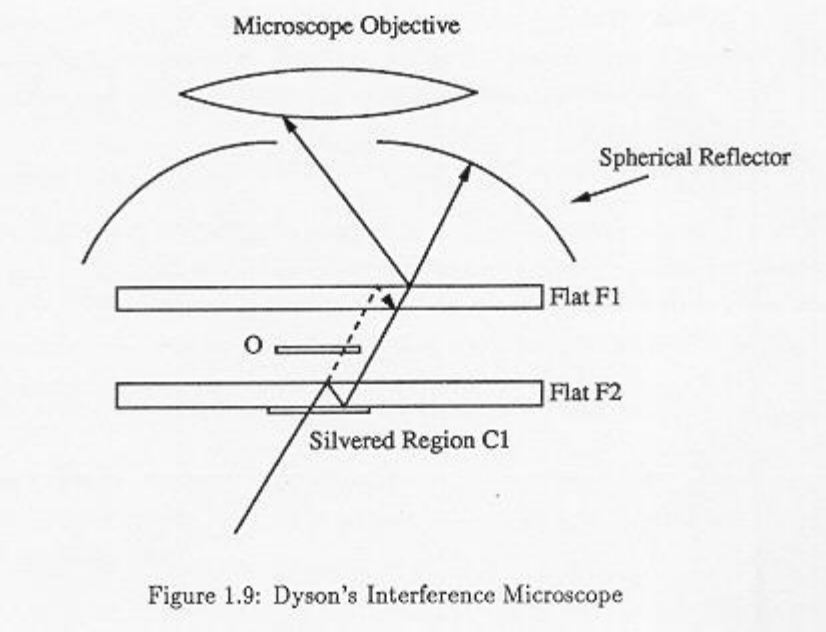

Figure 1.9: Dyson's Interference Microscope

2.3 Coherent Differentiation and Integration Technique

In this last section we describe a process capable of imaging phase variations with no limit as to their size. The usual problem with phase object imaging is that of phase redundancy; suppose a portion of the object has an optical path of 1.5λ relative to its surrounds. The resulting phase shift of the light field passing through the object is adequately described as though it had been shifted by only 0.5λ. This cyclic nature with which phase variations may be described, due to the periodic form of the sine function, is called redundancy and hampers even a process capable of linearly imaging the object phase as retardances greater than λ are once again perceived by linear systems as being small once more.

In the method of Sprague and Thompson [13], redundancy has been overcome. The phase object is placed in the object plane of a 6-f optical bench and in the Fourier Plane a *differentiating* filter [14] with transmittance

$$T(x) = C_1(x_0 - x) \tag{27}$$

is placed, where C_1 and x_0 are constants. This filter is essentially a wedge of decreasing transmittance along the x-axis of the frequency plane.

The resulting image intensity is given by

$$I(\alpha) = \left| \left[\frac{x_0}{f} + ik \frac{d\phi(-\alpha)}{d\alpha} \right] e^{ik\phi(-\alpha)} \right|^2 \tag{28}$$

where f is the focal length of the 6-f system lenses, and α is the image plane co-ordinate. This image is recorded on a photographic negative and a positive transparency taken. If the slope of the density vs log(exposure) curve of the exposure for the negative process is γ_n, and for the positive process γ_p, then with the condition that $\gamma_n \gamma_p = 1$ we have a resulting transmittance of

$$t(\alpha) = \frac{x_0}{f} + ik \frac{d\phi(-\alpha)}{d\alpha} \tag{29}$$

This transparency is used as the object in a separate optical processor, and is placed in a phase matched liquid gate to eliminate possible phase changes arising from the object relief image []. In the Fourier plane we now wish to use an integration filter to recover the phase φ(α) of the object, the ideal filter having a transmittance of

$$t(\nu) = \frac{D}{} \tag{30}$$

ν

where ν denotes distance along the axis of the frequency plane. This filter is physically unrealisable, having a singularity at the origin. In its place, the similar filter of transmittance

$$t(\nu) = iB \quad |\nu| < D \tag{31}$$

$$= \frac{D}{\nu} \quad |\nu| \geq D \tag{32}$$

is used, where B and D are constants. The outer parts of this filter perform the desired integration whereas the inner phase retarding region causes the image to be edge sharpened.

The resulting image intensity with this filter is described by

$$I(x) \cong \frac{E^2 x_0^{\,2}}{f^2} + \left(\frac{2Ex_0 k}{f} D \right) \Phi(\alpha) \tag{33}$$

where E is another constant.

The image intensity is thus a linear representation of the original object phase with no restrictions on the size of $\phi\alpha$. Two dimensional objects cause a problem in that the first differentiating filter can only differentiate the object along any one direction. However, a compromise is made by choosing this direction to lie at 45^0 to both the x and y axis. The great advantage of this method is that it can image phase objects with retardances greater than one wavelength of light linearly and without any redundancy effects. The principle disadvantage is the care required in the intermediate photographic stages, and the fabrication of the required filters. This method would be unsuitable where rapid indications of phase errors (in lens making for example) are required but should not be viewed detrimentally, it being a most skillful solution to the problem at hand.

2.4 Review

Starting from a historical perspective, many of the basic definitions and concepts of present day optical information processing have been introduced whilst reviewing the field of phase visualisation. Following the reasoning of Zernike, the essential differences between the spectra of phase objects and their amplitude object counterparts has been defined and, if the phase retardance is low, shown to be merely a constant additional phase term over all but the zero spectral order. The reader may consult section 35 of [7] for a summary of yet further visualisation techniques, those presented in this chapter serving mainly as an introduction to the subject.

3 Thesis Outline

The objectives of this project will now be defined, followed by a guide to the subjects of each chapter of this thesis. This project investigates the importance of phase in coherent optical information processing operations, an objective which has been subdivided into two regions of investigation. The objectives of this project are

1. To perform an in-depth analysis of the `phase contrast' phase visualisation operation on both the spectrum and image of a general phase object.

2. To investigate the use of phase-only spatial frequency filters for use in a classical matched correlator system. Further, to implement such filters on an electronically addressed spatial light modulator (SLM) currently in use within the Department of Physics of the University of Edinburgh.

Chapters one, two and three are concerned with fulfilling the first objective whose principal reason for being was to provide a thorough grounding in the concepts involved in phase-only processing. Study into phase-only correlation within the Applied Optics Group at the University of Edinburgh was initiated by Ranshaw [25], who performed a very limited set of experiments using a low resolution, 16×16 element spatial light modulator (cf

chapter four). The results produced were of rather low quality, although it must be stated that Ranshaw's experiment on optical correlation was never intended to be anything more than a scratch on the surface of the subject. In order to fully realise the potential of the 16×16 SLM as a phase modulator a much more extensive study was required. This work forms the basis of the majority of this thesis. Effective investigation into this area requires development along several fronts, namely

1. **The manufacture of a high quality phase-modulating SLM.**
2. **Development of a suitable computational framework within which both filter design and simulated correlations may be performed.**
3. **Precise manufacture and computational representation of the target objects and filters used.**
4. **Development of efficient filter computation algorithms.**
5. **Useful information extraction techniques for both simulated and experimental data.**

4 Summary of Chapters

Within the context of phase object visualisation, one particularly simple spatial filtering operation - that of the phase contrast technique - has been shown capable to result in an image intensity which is linearly proportional to the retardance of the phase object. This work forms the basis of chapter one. In the next chapter, the approximations used to examine the effect of the phase contrast filtering operation are reviewed in detail and an alternative mathematical framework for such an investigation is detailed. Chapter three utilises the ideas of the preceding chapter to draw several important conclusions on the range validity of the `weak phase' approximation.

The emphasis is changed in chapter four to the idea of phase-only filtering in classical matched correlator system where practical filters are discussed. Most practical phase-only filters, including correlation filters, are binary in nature and as such have relatively simple Fourier Transformation properties. Chapter five introduces the spatial light modulator used in this project to perform phase-only correlation and chapter six details several revisions to the construction procedure of this device. A computational framework for the simulation of the optical correlator system and filter calculation requirements is described in chapter seven. Chapter eight compares the results of computer simulation with actual binary phase-only correlations undertaken with a spatial light modulator fabricated according to the procedures of chapter six. Due to the large scope of this thesis, suggestions for continued investigation are clearly made within the relevant chapters although these are drawn together in the final chapter, chapter 9, together with a consideration of future work.

Footnotes:

[1]**The Dutch spectacle maker Hans Lippershey is usually credited with the invention of the telescope a few years earlier.**

[2]**The degree to which illumination coherence occurs in a microscope is discussed in `Born and Wolf' section 10.5.2. but it is noted here partial coherence can readily be achieved.**

File translated from T_EX by T_TH, version 3.02.
On 27 Oct 2001, 23:41.